

1 Towards a Pixel TPC part II: particle identification
2 with a 32-chip GridPix detector

3 M. van Beuzekom^a, Y. Bilevych^b, K. Desch^b, S. van Doesburg^a,
4 H. van der Graaf^a, F. Hartjes^a, J. Kaminski^b, P.M. Kluit^a,
5 N. van der Kolk^a, C. Ligtenberg^a, G. Raven^a, J. Timmermans^a

6 ^a*Nikhef, Science Park 105, 1098 XG Amsterdam, The Netherlands*

7 ^b*Physikalisches Institut, University of Bonn, Nussallee 12, 53115 Bonn,*
8 *Germany*

9 **Abstract**

10 A Time Projection Chamber (TPC) module with 32 GridPix chips was con-
11 structed and the performance was measured using data taken in a test beam
12 at DESY in 2021. The analysed data were taken at electron beam momenta
13 of 5 and 6 GeV/c and at magnetic fields of 0 and 1 Tesla(T). Part I of the
14 paper has described the construction, setup and tracking results.

15 The dE/dx or dN/dx resolution for electrons in the 1 T data per meter
16 of track length with 60% coverage was measured to be 3.6% for the dE/dx
17 truncation method and 2.9% for the template fit method using the successive
18 distances between the hits.

19 The single electron efficiency at high hit rates was studied. For hit rates
20 up 1.4 kHz per chip a reduction of at most 0.6% in the relative efficiency was
21 measured.

22 Hit bursts due to highly ionising particles were characterized.

23 The resolution in the precision plane as a function of the incident track
24 angle was measured in the $B = 1$ T data using reconstructed circle tracks.

*Corresponding author, Telephone: +31 20 592 2000
Preprint submitted to Nuclear Instruments and Methods A
Email address: s01@nikhef.nl (P.M. Kluit)

25 The resolution in the precision plane is - as expected - independent of the
26 incident angle ϕ within an uncertainty of $16 \mu\text{m}$.

27 The projected particle identification (PID) performance of a GridPix
28 Pixel TPC in the proposed ILD experiment at a future ILC e^+e^- collider
29 was presented using the $B=1$ T test beam results for the measured electron
30 PID resolution. The expected pion-kaon PID separation for momenta in the
31 range of 2.5-45 GeV/c at $\cos\theta = 0$ is more than $5.5(4.5)\sigma$ for the template
32 fit (dE/dx truncation) method.

33 *Keywords:* Micromegas, gaseous pixel detector, micro-pattern gaseous
34 detector, Timepix, GridPix, pixel time projection chamber

35 1. Introduction

36 As a step towards a Pixel Time Projection Chamber for a future collider
37 experiment [1], [2], a module consisting of 32 GridPix chips based on the
38 Timepix3 chip was constructed. The GridPix chips have a very fine granu-
39 larity of 256×256 pixels of $55 \times 55 \mu\text{m}^2$ and a high efficiency about 85% to
40 detect single ionisation electrons.

41 The 32-GridPix chip detector was put in a test beam at DESY and com-
42 plemented with two sets of Mimosas26 silicon detector planes. The analysed
43 data were taken at electron beam momenta of 5 and 6 GeV/c and at magnetic
44 fields of 0 and 1 T.

45 A description of the construction of the GridPix TPC module, the test
46 beam setup and data taking conditions can be found in part I of our paper
47 [3]. The paper explains the track reconstruction procedure and the precise
48 TPC tracking results that were obtained.

49 In the following sections the analysis results for different topics will be
50 presented. Firstly, the particle identification performance using dE/dx or
51 dN/dx will be measured. Secondly, the single electron efficiency at high
52 hit rates will be determined. Thirdly, the characterisation of large hit bursts
53 caused by highly ionising particles will be presented. Fourth, the resolution in
54 the precision plane as a function of the incident track angle will be measured.
55 Finally, the projected particle identification performance for a Pixel TPC in
56 the proposed ILD experiment at ILC [4] will be presented and discussed.

57 **2. Particle Identification using dE/dx or dN/dx**

58 Particles can be identified by their characteristic energy loss per unit
59 of track length dE/dx loss and/or the number of primary clusters dN/dx
60 produced along the track. In a GridPix detector one can measure the number
61 of hits produced along the track and their relative distance.

62 The distribution of the number of TPC track hits per chip for the $B = 0$
63 T and for the $B = 1$ T data sets are a starting point for a measurement of
64 the dE/dx or dN/dx performance. As was discussed in part I of the paper
65 [3], the mean number of hits is measured to be 124 and 89 in the $B = 0$ T
66 and 1 T data sets respectively. The most probable values are respectively 87
67 and 64.

68 In order to measure the track performance of dE/dx or dN/dx , a track
69 selection was applied selecting tracks crossing the central chips - defined in
70 [3]. The individual chips were calibrated to give the same mean number of
71 hits per chip. By combining the hits associated to the track from several
72 events, a new 1 m long track was formed. The 1 m long track has a coverage

73 of 60% because inactive regions (chip edges and e.g. guard) were included.

74 By applying different analysis methods, the dE/dx or dN/dx resolution
75 can be measured from data.

76 Both methods project the hits along the track in the xy plane. This gives
77 a distribution of hits as a function of the distance along the track in pixels.
78 The first method rejects large multi-electron clusters with more than in total
79 6 hits in 5 consecutive pixel bins. Finally, a dE/dx truncation at 90% is
80 performed using samples of 20 pixels; so the 10% largest dE/dx values are
81 removed and dE/dx re-estimated. This method does not fully exploit the
82 full granularity of the pixel TPC.

83 The second method exploits the distribution of the minimum distance
84 between consecutive hits in the xy precision plane. If only single electron
85 clusters were produced in a gas, one would expect an exponentially falling
86 distance distribution. Multi-electron clusters will give rise to a peak at low
87 distances that is smeared out by the transverse diffusion process. The slope
88 of the exponential distribution is proportional to the dN/dx i.e. the clusters
89 produced by the traversing beam electron. The long Landau tail in the
90 dE/dx distribution is coming from the multi-electron clusters that will peak
91 at low distances.

92 Using a large number of tracks, it is possible to measure from data the
93 shape of the minimum distance distribution. At distances above approxi-
94 mately 10 pixels the distribution follows an exponential distribution - see
95 Fig 5.15 in [2]. At lower distance, weights for the $B=0$ T and 1 T data are
96 determined and applied to ensure an exponential distribution over the whole
97 range.

98 Finally, per 1 m of track length, a fit to the distance distribution in data
99 is performed with the following template function:

$$N(d_{xy}) = N_0 \text{weight}(d_{xy}) e^{-\text{slope} \cdot d_{xy}}, \quad (1)$$

100 where d_{xy} is the minimum distance of the hits in the precision plane (xy) .
101 The slope and N_0 - normalisation - are left free in the per track fit, the
102 weights for the $B = 0$ and 1 T data are fixed using the whole data set.

103 The test beam data provide a dE/dx or dN/dx measurement for electrons.
104 The data were also used to perform a measurement of the response of a
105 minimum ionising particle (MIP) - here defined as a particle that produced
106 70% of the electron dE/dx . By dropping 30% of the hits associated to
107 the track and applying the two methods, the response of a MIP could be
108 measured and the linearity of the methods tested.

109 The relative resolution is defined as the r.m.s. of the distribution divided
110 by the mean and the results are shown in Table 1. The resolution of the $B =$
111 1 T data is about 40% better than the $B = 0$ T data. This is consistent with
112 the smaller fluctuations that are present in the distributions of the number
113 of hits per chip in the $B = 1$ T data [3]. The template fit method has in the
114 $B = 1$ T data a 20% better performance than the dE/dx truncation method.
115 One might argue that with more diffusion the results from the template fit
116 method will move more towards the results of the dE/dx truncation method.
117 Note however that the diffusion contribution to the track resolution in the
118 1 T data is already sizable compared to the pixel size and varies between
119 85-150 μm .

120 The results for the 1 T data are shown in Fig. 1 for electrons and MIPs
121 for the dE/dx truncation and template fit methods. The unit of the fitted

Table 1: dE/dx or dN/dx resolution for different methods and data sets

Method	$B= 0$ T [%]	$B= 1$ T [%]
dE/dx truncation	6.0	3.6
template fit	5.4	2.9

122 slope is inverse (pixel) distance, as is clear from the formula in Eq. 1. The
 123 linearity - defined as the mean MIP response divided by the mean electron
 124 response divided by 0.7 - was measured to be 1.03 for method 1 and 1.07
 125 for method 2. This value is slightly different from 1, and can be corrected
 126 for by scaling the expected values for different particles as a function of the
 127 measured momentum.

128 The dE/dx or dN/dx result of the 32-chip GridPix detector for electrons
 129 is impressive. It has currently, the best resolution per meter of track length
 130 of constructed TPCs running at atmospheric pressure - and demonstrates
 131 the particle identification capabilities of a GridPix Pixel TPC.

132 sectionSingle electron efficiency at high hit rates

133 The efficiency of the GridPix device to detect a hit in a high (low) rate
 134 environment is measured comparing the mean time over threshold (ToT) for
 135 low and high rate runs at B fields of 0 and 1 T. The mean ToT is sensitive
 136 to the single electron efficiency of the detector. In order to extract a precise
 137 result, hits associated to TPC tracks were used. The track selection is the
 138 same as in section 2. The analysed runs for the $B = 0$ T data set were runs
 139 6916, 6934 and 6935 and for the $B = 1$ T data set runs 6969 and 6983.

140 For each run the mean ToT values were measured in the interval between
 141 0.15 and 1.4 μ s. These cuts were applied to remove the noise and the upper

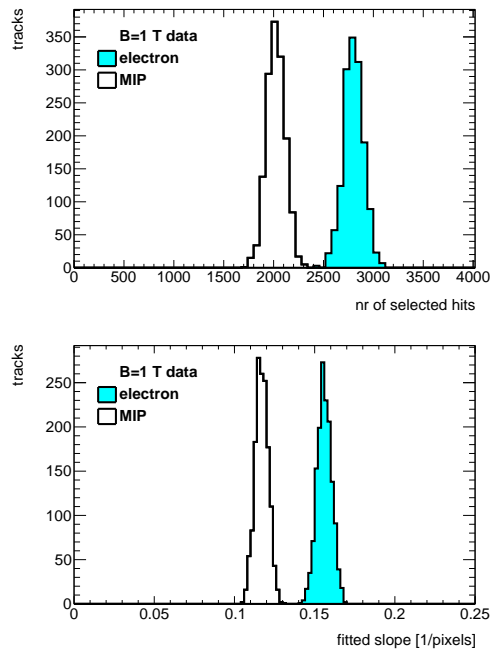


Figure 1: Distribution of the number of selected hits for the dE/dx truncation method (left) and the fitted slope for the template fit method (right) for an electron (light blue shaded) and for a MIP using 1 m long tracks with 60% coverage for the $B = 1$ T data.

142 tail of the distribution.

Table 2: Mean ToT and rates for different runs

run	B	ToT1	ToT2	triggers	run time	Hits1	Hits2	trig rate	Rate1	Rate2
	[T]	[μ s]	[μ s]	10^3	[10^3 s]	10^6	10^6	[Hz]	[hits/s]	[hits/s]
6916	0	0.628	0.653	16.8	23.2	6.25	13.1	0.72	269	565
6934	0	-	0.651	7.34	2.41	-	20.5	30.4	-	8479
6935	0	0.620	-	7.39	2.41	6.95	-	30.6	2878	-
6969	1	0.650	0.666	7.94	13.8	1.93	2.16	0.57	139	156
6983	1	0.657	0.678	6.79	2.83	11.6	14.1	24.1	4110	4986

143 The results for the measured average ToT for different runs and hit
144 rates are summarised in Table 2. ToT1(2) denotes the mean ToT for up-
145 per and lower half (in x) of the module and Hits1(2) corresponds to number
146 of recorded raw hits. The mean Rate1(2) was calculated dividing the total
147 number of raw hits by the total run time. The instantaneous rate in runs
148 6934, 6935 and 6983 taken at 5 GeV/c is about a factor 3 higher (due to the
149 duty cycle of the machine). For the $B = 0$ T data, two high rate runs 6934
150 and 6935 taken at a beam momentum of 5 GeV/c had to be analysed be-
151 cause the beam crossed either the upper or the lower part of the module and
152 therefore no measurement could be performed (denoted by -). The statistical
153 uncertainties are negligible.

154 The relative change in the mean ToT for the $B = 0$ data is -1.2% (upper)
155 and -0.3% (lower). In this case the rate goes up to 8.5 kHz for 6 chips or 1.4
156 kHz per chip. The relative change in the mean ToT for the $B = 1$ T data
157 is +1% (upper) and +1.7% (lower) The rate goes up to 5 kHz for 6 chips or

158 1.2 kHz per chip.

159 The relative change in the mean ToT can be related to the relative change
160 in the single electron efficiency $\delta\epsilon/\epsilon$ by:

$$\delta\text{ToT}/\text{ToT} = d \delta\epsilon/\epsilon. \quad (2)$$

161 The derivative d is about 0.5 at the mean working point of $\text{ToT}=0.65 \mu\text{s}$ and
162 is determined from the measured efficiency-ToT curve in [2].

163 This means that the relative efficiency is stable at the level of +0.9% (B
164 = 1 T) and -0.6% ($B = 0$ T) for hit rates up to 1.2 (1.4) kHz per chip. To
165 conclude, running at hit rates up 1.4 kHz per chip gives a reduction of at
166 most 0.6% in the relative efficiency.

167 **3. Characterisation of hit bursts**

168 In event displays hit burst caused by highly ionising particles (e.g. alpha
169 particles or delta electrons) can be observed. An example event is shown in
170 Fig. 2. A large variety of hit patterns can be observed: large radii (open)
171 circles, smaller size radius circles from low momentum particles, curlers and
172 more confined bursts. A track with a momentum of 1 MeV/c will have a
173 typical radius of 60 pixels. A Pixel TPC is well suited to study and charac-
174 terize these typical hit bursts. After a reconstruction and characterisation of
175 the burst it is possible to reject the hits associated to the bursts. This will
176 improve the measurement of the track parameters in the final track fit. .

177 To study the hit bursts, the data of run 6969 - taken at a 5 GeV/c beam
178 momentum in a $B = 1$ T field - were analysed. Bursts were selected with
179 more than 100 hits in a radius of 50 pixels around the burst centre within

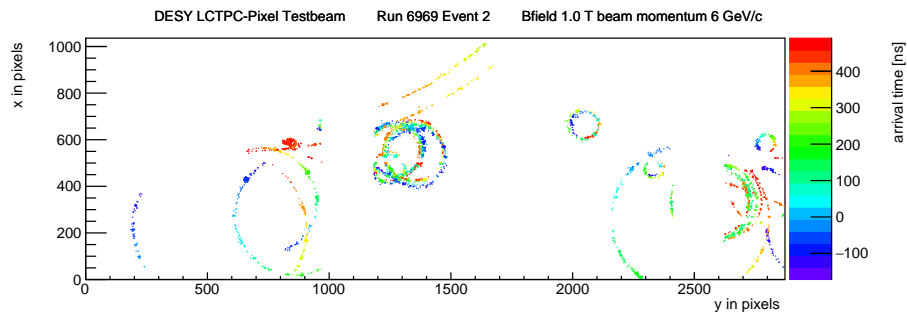


Figure 2: An event display for run 6969 event 2 taken at a 5 GeV/c beam momentum in a $B = 1$ T field. The hits are shown in the xy plane in colour the time of arrival is shown.

180 a time window of 200 ns around the mean time. The mean position in xy
 181 and the mean time of the burst were iteratively estimated. The bursts were
 182 characterized by the number of associated hits, the radius in which 90% of the
 183 hits are found (radius90) and the time in which 90% of the hits are detected
 184 (time90). The stacked distributions for the radius90 and time90 variables for
 185 different burst sizes are shown in Fig. 3.

186 It is clear that the radius90 and time90 distributions broaden as a function
 187 of the number of hits. In particular the time90 distribution develops a long
 188 tail for high number of hits. Note that hits that end up on the same pixel
 189 within the Timepix3 pixel dead time of 475 ns will not be recorded, so part
 190 of the core of the burst might remain undetected. Still the detector is able
 191 to record hit bursts of at most 7854 hits in a 50 pixel radius. The largest hit
 192 burst in run 6969 had 3180 hits.

193 For high momentum tracking it is important to cut tightly on the track
 194 residuals in xy and z . In particular the cut in z reduces the impact of bursts
 195 in the $B = 1$ T data. In the pattern recognition one could run a burst finding

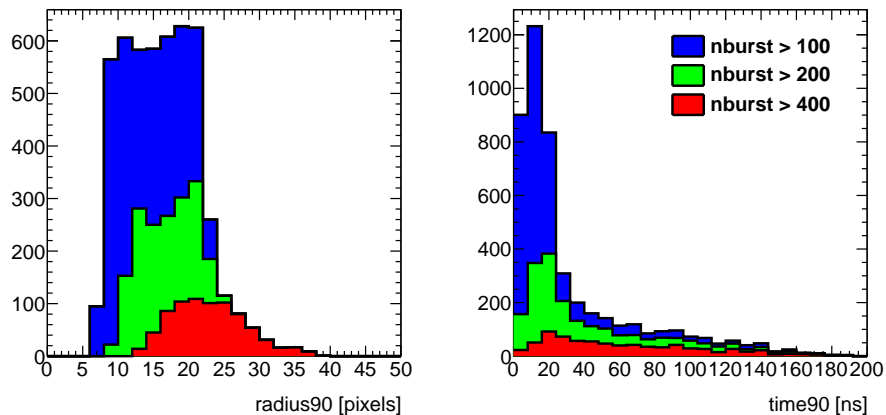


Figure 3: The stacked distributions for radius90 and time90 for burst with more than 100 (blue), 200 (green) and 400 (red) hits for run 6969.

196 algorithm and down weight in the track fit the hits associated to bursts. This
 197 will remove biases and improve the track parameter estimation.

198 4. Track resolution as function of the angle

199 The resolution in the precision plane as a function of the incident angle of
 200 the track will be measured in the $B = 1$ T data set. For a pad based readout
 201 system the resolution has a strong dependence on the incident angle see e.g.
 202 [5]. The resolution is best if the incident track angle is parallel to the strip
 203 direction.

204 For a GridPix pixel TPC - with squared pixels - the resolution is expected
 205 to be independent of the incident angle. In order to test experimentally
 206 this hypothesis, reconstructed circle tracks were selected. Examples of circle
 207 tracks can be observed in the event display shown in Fig. 2. For circles, the
 208 incident ϕ angle of the track depends on the position of the individual hits

209 on the circle in the xy plane. The range of ϕ angles depends on the radius.
 210 For radii smaller than 500 pixels a large ϕ range can be probed. Using the
 211 residuals in the xy plane, it is possible to measure the resolution of the hits
 212 as a function of the incident ϕ angle of the track.

213 A dedicated pattern recognition program was written to find and fit mul-
 214 tiple circles in an event. To find candidate circles, a Hough transform was
 215 used to find the centre of the circle in the xy plane. In the circle fit, the reso-
 216 lution in xy was estimated to be about 4 pixels and in z it was 1 mm. Outlier
 217 hits at more than 2.5 standard deviation were iteratively rejected. For the
 218 selection of circles it was required that the fit $\chi_{xy}^2/d.o.f.$ and $\chi_z^2/d.o.f.$ was
 219 less than 5. Finally, the radius of the circle had to be larger than 50 pixels
 220 (corresponding to a momentum cut of 0.8 MeV/c), at least 20 hits should
 221 lie on the circle. The total ϕ span of the selected hits on the circle should
 222 be at least 1 rad. The hits with ϕ values below $\pi/8$ and above $15\pi/8$ were
 223 removed.

224 The selected data set has 973 circles, with a mean radius of 155 pixels
 225 and a mean number of hits of 194. Because the resolution depends on the
 226 radius (i.e. the momentum) and small radii span a large ϕ range, the data
 227 were re-weighted as a function of the circle radius. Finally, the resolution in
 228 xy was extracted - using a Gaussian fit to the track residuals in the range
 229 of $\pm 2\sigma$ around the centre. The fitted resolution in xy as a function of the ϕ
 230 incident angle of track for the hits on the circle is shown in Fig. 4.

231 A curve was fitted to the data using the following expression:

$$\sigma_{xy} = \sigma_0 + \sigma_1 \cos \phi, \quad (3)$$

232 where σ_0 and σ_1 were left free. The fit result yielded $\sigma_0 = 0.241$ mm and

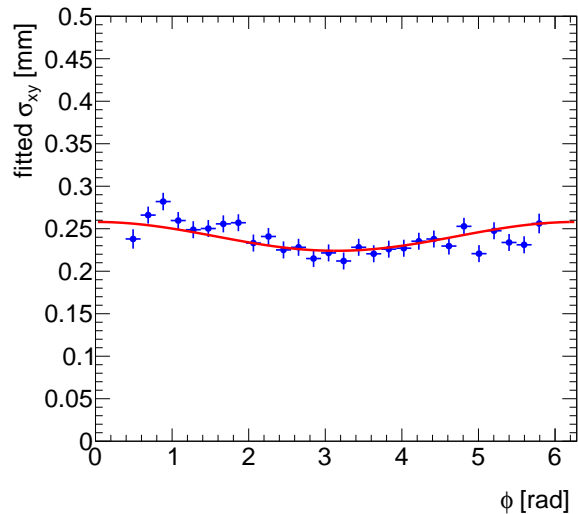


Figure 4: The fitted resolution in xy as a function of the ϕ incident angle of the hits on the circle. The fitted curved in red is given in Eq. 3.

233 $\sigma_1 = 0.016$ mm and describes the modulation observed in the data.

234 It can therefore be concluded that the resolution in the precision plane is
 235 independent of the incident angle ϕ within an uncertainty of $16 \mu\text{m}$.

236 *4.1. Projected particle identification performance for a Pixel TPC in the pro-*
 237 *posed experiment ILD at a future ILC*

238 The particle identification (PID) performance of electrons in the test
 239 beam for momenta of 5-6 GeV/c was measured to 2.9% for the template
 240 fit and 3.6% for the dE/dx truncation method at $B = 1$ T for 1 m long
 241 tracks with 60% coverage. The TPC of the proposed ILD detector [4] has
 242 an inner radius of 329 mm, an outer radius of 1770 mm and a half length
 243 of 2350 mm. In the ILD TPC this will correspond to an expected electron
 244 PID resolution of 2.4% (fit) and 3% (truncation) at polar a angles of $\theta = \pi/2$

245 ($\cos \theta = 0$) and a track length (tlength_0) of 1441 mm. The PID resolution
 246 for different particles can be written as:

$$\sigma_i = \sigma_e \sqrt{\text{tlength}_0 E_e} / \sqrt{\text{tlength} E_i}, \quad (4)$$

247 where tlength is the track length and E_i is the expected energy loss for
 248 particle i (electron = e , muon = μ , pion = π , kaon = K , proton = p).
 249 Clearly, the best PID resolution will be reached for the largest track length,
 250 which corresponds to $\cos \theta = 0.85$ in ILD.

251 The ILD parametrisations of the energy loss for different particles as a
 252 function of the momentum were used as given in [6]. They are based on
 253 full simulations of the ILD TPC operated with a T2K gas and running at
 254 atmospheric pressure. The PID separation in numbers of standard deviations
 255 w.r.t. the π hypothesis for the e , K and p is defined as:

$$\text{separation}_i = |E_i - E_\pi| / \sigma_\pi. \quad (5)$$

256 In Fig. 5, the separation of electrons, kaons and protons w.r.t. pions
 257 are shown as a function of the momentum of the particle for projected ILD
 258 electron PID resolutions of 2.4 and 3% at $\cos \theta = 0$. The expected pion-kaon
 259 PID separation for momenta in the range of 2.5-45 GeV/c at $\cos \theta = 0$ is
 260 more than $5.5(4.5)\sigma$ for the two resolution scenarios. At a momentum of 100
 261 GeV/c the separation is still $3.0(2.0)\sigma$. Protons can be separated from pions
 262 for momenta in the range of 2.5-100 GeV/c with more than $6.0(4.8)\sigma$.

263 It is clear from the above that a GridPix Pixel TPC in ILD will provide
 264 powerful particle identification.

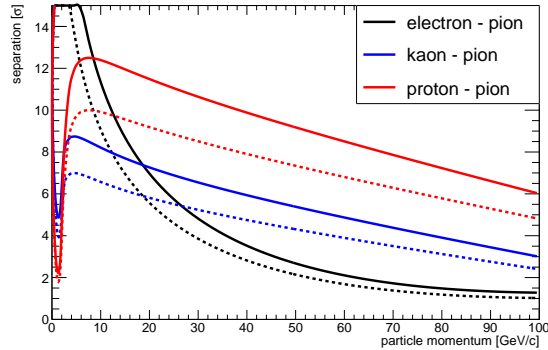


Figure 5: The projected PID separation for a GridPix TPC in ILD for electrons, kaons and protons w.r.t. pions at $\cos\theta = 0$. The continuous lines correspond to an electron PID resolution of 2.4% and the dashed to 3%.

265 5. Conclusions and outlook

266 A Time Projection Chamber (TPC) module with 32 GridPix chips was
 267 constructed and the performance was measured using data taken in a test
 268 beam at DESY in 2021. The analysed data were taken at electron beam
 269 momenta of 5 and 6 GeV/c and at magnetic fields of 0 and 1 T.

270 The precise tracking results for the module were presented in part I of
 271 the paper [3].

272 The dE/dx or dN/dx resolution for electrons of momenta 5 and 6 GeV/c
 273 in the 1 T data for a 1 m track with 60% coverage was measured to be 3.6%
 274 for the dE/dx truncation method and 2.9% for the template fit method. This
 275 result is impressive and is currently, the best resolution per meter of track
 276 length of constructed TPCs running at atmospheric pressure.

277 The single electron efficiency at high hit rates was studied. For hit rates
 278 up 1.4 kHz per chip a reduction of at most 0.6% in the relative efficiency was

279 measured.

280 Hit bursts due to highly ionising particles were characterized showing the
281 pattern recognition capabilities of a GridPix Pixel TPC.

282 The resolution in the precision plane as a function of the incident track
283 angle was measured in the $B = 1$ T data using reconstructed circle tracks. It
284 was demonstrated that the resolution in the precision plane is - as expected
285 - independent of the incident angle ϕ within an uncertainty of $16 \mu\text{m}$.

286 The projected particle identification performance of a GridPix Pixel TPC
287 in ILD was presented using the $B = 1$ T test beam results for the measured
288 electron PID resolution. The expected pion-kaon PID separation for mo-
289 menta in the range of 2.5-45 GeV/c at $\cos \theta = 0$ is more than 5.5 (4.5) σ for
290 the template fit (dE/dx truncation) method.

291 It is clear that a GridPix Pixel TPC in ILD will provide powerful parti-
292 cle identification. At the CEPC collider a Pixel TPC is proposed, because
293 of the precise tracking and particle identification capabilities. The GridPix
294 detector will be further tested and developed for a TPC that could be in-
295 stalled in a heavy ion experiment at the Electron Ion Collider. In the DRD1
296 collaboration at CERN a GridPix Pixel TPC is also part of the research
297 program.

298 **Acknowledgments**

299 This research was funded by the Netherlands Organisation for Scientific
300 Research NWO. The authors want to thank the support of the mechanical
301 and electronics departments at Nikhef and the detector laboratory in Bonn.
302 The measurements leading to these results have been performed at the Test

303 Beam Facility at DESY Hamburg (Germany), a member of the Helmholtz
304 Association (HGF).

305 **References**

306 [1] M. Lupberger, Y. Bilevych, H. Blank, D. Danilov, K. Desch, A. Hamann,
307 J. Kaminski, W. Ockenfels, J. Tomtschak, S. Zigann-Wack, To-
308 ward the Pixel-TPC: Construction and Operation of a Large Area
309 GridPix Detector, IEEE Trans. Nucl. Sci. 64 (5) (2017) 1159–1167.
310 doi:10.1109/TNS.2017.2689244.

311 [2] C. Ligtenberg, A GridPix TPC readout for the ILD experiment at the
312 future International Linear Collider, Ph.D. thesis, Free University of
313 Amsterdam (2021).
314 URL https://www.nikhef.nl/pub/services/biblio/theses_pdf/thesis_CLigtenberg.p

315 [3] M. van Beuzekom, et al., Towards a Pixel TPC part I: construction and
316 test of a 32-chip GridPix detector, submitted to Nucl. Instrum. Meth.
317 A.

318 [4] T. Behnke, J. E. Brau et al., eds. The International Linear Collider.
319 Technical Design Report. Vol. 4: Detectors. Linear Collider Collabora-
320 tion, 2013. arXiv: 1306.6329. doi:10.48550/arXiv.1306.6329.
321 URL <https://www.linearcollider.org/>

322 [5] LCTPC Collaboration, David Attié et al., A Time Projection Cham-
323 ber with GEM-Based Readout, Nuclear Instruments and Methods in
324 Physics Research. Section A: Accelerators, Spectrometers, Detectors

325 and Associated Equipment 856, 1 (2017), 109–118. arXiv:1604.00935v1,
326 doi:10.1016/j.nima.2016.11.002.

327 [6] iLCSoft, Linear Collider Software,
328 URL <https://github.com/iLCSoft/MarlinReco/blob/master/Analysis/PIDTools/>,
329 based on version v02-02-01.